Polym. Bull. (2012) 68:2199–2217
DOI 10.1007/s00289-012-0722-1

ORIGINAL PAPER

Evaluation of polypropylene/montmorillonite nanocomposites as food packaging material

Gislene Zehetmeyer · Rosane M. D. Soares · Adriano Brandelli · Raquel S. Mauler · Ricardo V. B. Oliveira

Received: 9 December 2011 / Revised: 9 February 2012 / Accepted: 20 February 2012 /
Published online: 25 March 2012

Abstract The aim of this study was to use nanocomposites of polypropylene (PP) and montmorillonite (MMT), prepared by melt intercalation in a twin-screw extruder, as a food packaging material. The nanocomposites were evaluated by thermal, mechanical, and morphological analyses. Measurements of oxygen and water vapor permeability were also conducted to the nanocomposites. Besides, orange juice was used as modeling food and its physical–chemical and microbiological properties were determined. Despite of no significant changes in tensile properties were observed to the nanocomposites, the impact strength presented a substantial enhancement and the rigidity as well. Besides, MMT have shown a high capacity to improve oxygen barrier properties of PP. Electronic microscopy revealed certain homogeneity, showing some MMT-exfoliated lamellae in the PP matrix. Regarding the package efficacy, the orange juice quality was maintained after 10 days of storage. Concluding, this study seems to clarify a little more the claimed efficiency of nanocomposites as food packing materials.

Keywords Nanocomposites · Polypropylene · Montmorillonite · Permeability · Food packaging

G. Zehetmeyer · R. M. D. Soares · R. S. Mauler · R. V. B. Oliveira (✉)
Institute of Chemistry, Universidade Federal do Rio Grande do Sul (UFRGS),
Porto Alegre, RS, Brazil
e-mail: ricardo.oliveira@iq.ufrgs.br

A. Brandelli
Institute of Food Science and Technology, Universidade Federal do Rio Grande do Sul (UFRGS),
Porto Alegre, RS, Brazil

Introduction

Over the last three decades, the use of polymers as food packaging materials has increased enormously due to their advantages over other traditional materials [1]. Despite of this, food packaging yet represents a market of high potential for polymer materials. The continued quest for innovation in food and beverage packaging is mostly driven by consumer needs and demands influenced by changing global trends. In recent years, consumers have shown preferences for fresh, tasty, and minimally processed food products with a prolonged shelf life and new food packaging systems have been developed in response to these trends [2].

Nanocomposite packages are predicted to make up a significant portion of the food packaging market in the near future. Polymer nanotechnology is actually developed mainly to improve barrier performance belonging to gases such as oxygen and carbon dioxide. It is proved also to enhance the barrier performance to ultraviolet rays, as well as to add strength, stiffness, dimensional stability, and high temperature durability [3–6]. In addition, packaging with improved barrier properties extends the shelf life of foodstuffs, preventing humidity or substances such as oxygen, ethylene, or strange flavors interacting with the food. Preventing contact between these substances and food, decreases the risk of adverse reactions that could reduce the organoleptic and/or sanitary quality of the product [2]. A major application of commercial interest is to obtain films with better barrier properties, leading to reduction of permeability and the possibility of new applications or even aiming at the reduction of the economic and environmental cost of packaging.

Polypropylene/montmorillonite (PP/MMT) nanocomposites are one of the most commonly used, prepared to get numerous improvements to their properties [7, 8]. The incorporation of small amounts of inorganic material, such as MMT, has been used to improve the properties of polymeric materials [9, 10]. This approach aims to achieve an improvement in mechanical strength, thermal stability, and barrier properties [11, 12]. In this context, PP/MMT nanocomposites display an attractive combination of low cost and great versatility in terms of properties, applications, and recycling [8, 13].

The main method to obtain nanocomposites is melt intercalation, and normally a twin-screw extruder is used [14]. The degree of enhancement of PP/MMT nanocomposite properties is related with the presence of strong interactions between the clay and the polymer chain, besides the diffusion of the polymeric chains into the clay layers [15, 16]. The hydrophilic surface of MMT usually is modified by ion exchange reactions with quaternary ammonium salts, containing long alkyl chains; thus there is a formation of an organic layer onto the clay surface, thereby reducing its polarity. This modification increases the compatibility between MMT and the chairs of nonpolar polymers, such as PP. So, the level of nanofiller dispersion in the PP matrix is thermodynamically favored. Indeed, in these systems, the clay/matrix interactions must be high enough to obtain an optimized morphology consisting in a major population of exfoliated clays with a strong interface toward the polymer matrix [17]. Three basic types of morphology are possible: agglomerates, intercalated, where the polymeric chains are inserted into the layers of the clay forming an orderly multilayer structure, and exfoliated, where the silicate layers are completely separated and dispersed in the polymer matrix [18].

The manufacture of films for packaging production requires a high-quality raw material, because the films have a high ratio between surface and volume and need to present a high degree of purity. A very interesting product is the PP/MMT films, which depending on the orientation of the PP chains, and MMT sheets can result in polymeric films with excellent barrier properties, stiffness, and mechanical resistance. Although a number of studies on nanocomposite PP/clay have been carried out, only few studies involving nanocomposites with the direct application in food packaging can be found in the literature. On this basis, the aim of this study is to study the incorporation of the MMT at different concentrations in PP matrix and, to develop a food package film with good exfoliation, which can lead to enhanced barrier, and mechanical properties. Also, orange juice was used in this study to simulate a real food package system.

Experimental

Materials

PP homopolymer with a melt flow index (MFI) of 3.5 g 10^{-1} min^{-1} (230 °C/2.16 kg) and density 0.905 g cm^{-3} (23 °C) was purchased from Braskem S.A, Brazil. The nanoclay mineral used was the MMT Cloisite® 15A, group of smectites, organically modified with a salt of alkyl quaternary ammonium, from Southern Clay Products. The orange juice used was 100% pure, freshly squeezed, unpasteurized from fruit of the variety Pear [*Citrus sinensis* (L.) *Osbeck*]. The oranges were obtained from CEASA, in the city of Porto Alegre, Brazil.

Preparation of the nanocomposites

Nanocomposites (with clay contents up to 5% by weight) were prepared by melt mixing using a co-rotation twin-screw extruder Coperion, model ZSK18 with a screw diameter of 18 mm and $L/D = 44$. The temperature profile (feed to die) was 165–190 °C, with a speed of 350 rpm and a constant feed rate of 5 kg h^{-1}. After processed, the nanocomposites were granulated in a granulator Sagec SG-35. The PP/MMT films were produced in planar sheet extruder Knödler OCS, model TYP-F2 50.2-U-ED 20, and the material was placed directly into the hopper of the extruder with a temperature profile (feed to die) of 200–240 °C, screw speed of 40 rpm and torque of 40–60 Nm. The films were produced with a thickness of ~ 25 μm for use in permeability tests and packing. In addition, the granular materials were also injected ion-molded (Battenfeld Plus 350), with a profile of temperature 220–230 °C and mold temperature of 50 °C according to ASTM D 4101-55b, as type I specimens (ASTM D 638).

Characterization of the nanocomposites

Differential scanning calorimetry (DSC)

Calorimetric measurements were done using a DSC Thermal Analyst 2100/TA Instruments, in a dry nitrogen atmosphere (50 mL min^{-1}). All samples (ca 10 mg)

were heated from ambient temperature to 220 °C and kept for 5 min to erase the thermal history. The samples were then cooled down to −30 °C and heated again until 220 °C. All runs were conducted with a heating rate of 10 °C min^{-1}. The crystallinity degree was determined using $\Delta H_m^0 = 190$ J g^{-1} for PP.

Dynamic mechanical analysis (DMA)

Dynamic mechanical experiments were carried out in a DMA Q800, TA Instruments, using single cantilever geometry. The injection-molded samples were heated from −30 to 150 °C, with heating rate of 3 °C min^{-1}, and the frequency was set to 1 Hz for all samples.

Thermogravimetric analysis (TGA)

The thermal stability evaluation was carried out using a thermogravimetric analyzer model QA 50 (TA Instruments). The samples were heated from 25 to 800 °C at the rate 10 °C min^{-1} under nitrogen atmosphere (50 mL min^{-1}).

X-Ray diffraction (XRD)

XRD measurements were performed using a Siemens D-500 diffractometer. Neat MMT powder and PP/MMT nanocomposites films were scanned in the reflection mode using an incident X-ray of Cu Kα ($\lambda = 1.54$ Å), at a step width of 0.05°s^{-1} from $2\theta = 1°$–35°. The dispersion of the layers in the nanocomposites, as well as the basal spacing of the clays, were estimated from the (*001*) diffraction.

Tensile test

Type I specimens were used according to ASTM D-638 (3.2-mm thick). The specimens were acclimatized for 24 h at 23 °C ± 2 with humidity 50% ± 5 before the tensile tests Emic universal test machine, DL 10.000, at a speed of 50 mm min^{-1} and base length of 50 mm, also according to standard ASTM D-638.

Izod impact strength

The izod impact tests were carried out at 23 °C using pendulum Ceast, Resilimpact 6545. The specimens suffered an impact of 2.75 J through a hammer with speed of 3.46 m s^{-1}. The tests were performed according ASTM D-256.

Transmission electron microscopy (TEM)

The specimens' morphologies were examined by TEM (JEOL JEM-1200 Ex II), which operated at an accelerating voltage of 80 kV. Ultra-thin specimens (70 nm) were cut from the middle section of injection-molded specimens in a direction perpendicular to the flow of the melt during the injection process. Cutting operations were done under cryogenic conditions with a Leica Ultracut UCT microtome

equipped with a glass knife at −80 °C. The cuts were placed onto 300 mesh Cu grids.

Oxygen permeability

The determination of oxygen permeability through PP/MMT films was obtained using an OX-TRAN 2/21 (Mocon, MH) at 23 °C and 0% relative humidity, in duplicate, according to ASTM F-1927. The detector used was a coulometric oxygen sensor. The test was terminated automatically after stabilization in the permeation and using synthetic air (20% O_2) as permeant gas.

Water vapor permeability

The determination of permeability to water vapor PP/MMT films was obtained using a PERMATRAN-W 3/33 (Mocon, MG) at 37.8 °C and 90% relative humidity, in duplicate, according to ASTM F-1249. The detector used was an infrared sensor, and the test was terminated automatically after stabilization in permeation.

Scanning electron microscopy (SEM)

SEM was carried out using a Scanning Electron microscope JEOL model JSM-5800 equipped with an EDX microanalysis system, operating at a voltage of 10 kV.

Orange juice production, storage, and physical–chemical analysis

Oranges, after selection and washing, were subjected to the process of juice extraction in a machine Walita. The juice was immediately transferred into a sterile glass container under sanitized conditions. Bags of pure PP and PP/MMT films with 75 cm^2 were prepared to store juice samples. Samples (60 mL) of fresh orange juice was poured into each package and sealed. Packages containing orange juice were stored in the absence of light and under controlled temperature. The samples were evaluated at least in duplicate for physical–chemical characteristics at time 0, and after 1, 2, 3, 4, and 10 days of storage. Physical–chemical analysis were carried out by investigating the following parameters: density at 20 °C, soluble solids in °Brix, total sugars, citric acid, insoluble solids, pH, ascorbic acid (AA) and sugars, according to the methodology of Association of Official Analytical Chemists (AOAC) [19].

Microbiological analysis

The microbiological analyses were performed according to the methodology proposed by American Public Health Association (APHA) [20]. Total counts of mesophilic bacteria were determined by the method of standard plate count, using plate count agar (PCA). Incubation of the samples was performed at 35 °C for 48 h. Total yeast and molds were enumerated using the surface plate method on the potato

dextrose agar (PDA), plus 10% tartaric acid. Incubation for total yeast and mold counts was performed at 25 °C for 5 days. Each test was performed in duplicate and results were expressed as colony-forming units (CFU) per milliliter. Total and fecal coliforms were determined by most probable number technique in the Brilliant Green broth at 2.0 g 10^{-2} mL^{-1} and EC broth, respectively [20]. After the readings of the tubes of lactose broth presumptive test for coliforms, the incubation was performed for 48 h at 36 °C for the determination of total coliforms, and 24 h at 44.5 °C for the determination of fecal coliforms.

Results and discussion

Characterization of PP–MMT nanocomposites

A summary of the main thermal transitions of PP and PP/MMT nanocomposites can be visualized in Table 1. It was observed that such temperatures did not change significantly when compared to pure PP.

The degree of crystallinity decreased (X_c), as a function of 2 wt% MMT content. The sample with 5 wt% MMT content presented a higher X_c, this behavior can be explained by changes in the crystalline phase that may influence the reinforcement ability of the clay on the nanocomposite [7]. It was also observed a constant crystallinity (about 60%), within the experimental error for all the specimens.

Figure 1a and b shows the dependence of the storage modulus (E'), loss modulus (E'') and tanδ as function of temperature, respectively. According a previous investigation [7], PP nanocomposites shows a small increase in their storage modulus, when compared to neat PP, indicating that the incorporation of clay in PP matrix promotes a good reinforcing effect in tensile properties.

However, an opposite effect was observed in this study, probably due to the poor interaction between the clay and the PP matrix, since the clay has not been modified. It is possible to observe that the addition of clay into the PP matrix did not contribute to significant changes in E' and E''.

Furthermore, the presence of fillers caused a small decrease in storage modulus, indicating that the filler did not act as a reinforcing material, in this case, these decreases in the modulus as function of MMT content can be explained by an increase in polymer chains mobility.

As expected, the nanocomposites loss modulus (E'') showed an increase in their values when compared to neat PP, and two major transitions were detected. The first one, at 13 °C, can be associated to the glass transition temperature (T_g) of the PP,

Table 1 Thermal properties of the neat PP and PP/MMT nanocomposites

Samples	T_m (°C)	T_c (°C)	X_c (%)
Neat PP	169	129	62
PP + 1% MMT	168	128	59
PP + 2% MMT	168	124	59
PP + 5% MMT	168	121	62

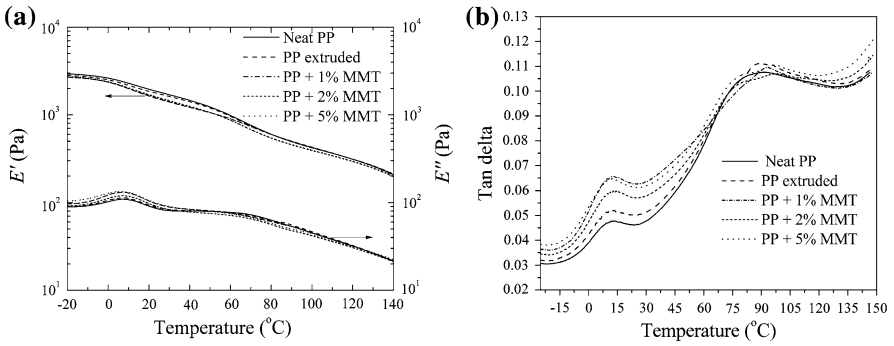

Fig. 1 **a** Storage (E') and loss (E'') modulus as function of temperature for PP and nanocomposites at different concentrations up to 5 wt%, and **b** tanδ as a function of temperature for neat PP and PP/MMT nanocomposites

and the transition at 86 °C can be related to the relaxations in the intracrystalline amorphous chains of the PP [21]. The tanδ curves for nanocomposites showed higher values than neat PP below T_g, indicating weak clay–polymer interactions. As can be observed, the dispersion of fillers into the PP matrix induced changes in mechanical and dynamic mechanical behaviors, probably due to modifications in chain mobility.

Table 2 shows the results of TGA, and these revealed that the MMT filler had some effect on the thermal stability of the nanocomposites. All nanocomposites showed higher initial thermal stability ($T_{10\%}$) compared to Neat PP, as well as $T_{50\%}$ (max rate), presenting a faster decomposition step. A previous investigation of Fu and Qutubuddin [4] suggested that the barrier properties of the nanoscale fillers were responsible for the enhancement of thermal stability of nanocomposites.

The degradation of PP in these conditions involves reactions which lead to main chain break and cleavage. These reactions result in smaller chains with radicals at their ends. The intermolecular radical transfer may originate internal radicals and then β scission occurs, leading to formation of volatile products and residues with unsaturated terminations [22].

According to Table 2, the clay addition into PP matrix improved its thermal stability. PP nanocomposites increased the initial decomposition temperature ($T_{10\%}$) compared to neat PP since MMT could have migrate to the surface forming a protecting barrier and blocking the release of gas during their decomposition, as a consequence, there is an increase in the PP degradation temperature [7]. Figure 2

Table 2 Results of TGA of PP and PP/MMT nanocomposites

Samples	$T_{10\%}$ (°C)	$T_{50\%}$ (°C)	Residue (%)
Neat PP	389	454	1.1
PP + 1% MMT	454	469	1.1
PP + 2% MMT	440	459	1.5
PP + 5% MMT	443	463	3.2

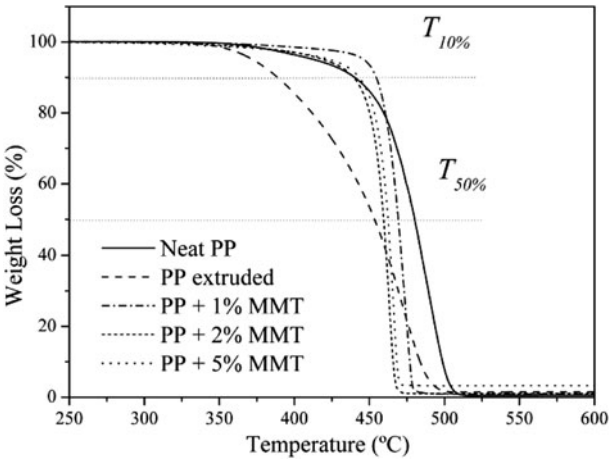

Fig. 2 TGA curves of the neat PP and PP/MMT nanocomposites

shows the TGA curves of pure PP and PP/MMT nanocomposites. The thermogravimetric curves demonstrated that the incorporation of clay into PP matrix improved its thermal stability. All the PP nanocomposites increased the initial decomposition temperature ($T_{10\%}$) compared to pristine PP, because the MMT form a protecting barrier when migrates to the surface, that avoid the release of gas from the decomposition, increasing the thermal stability of the material. The weight loss at 50% ($T_{50\%}$, Table 2) occurs for almost all samples at the same temperature (450 °C) except for PP extruded. All nanocomposites and pristine PP have almost the same final decomposition temperature ($T_{50\%}$). However, the nanocomposites presented an accentuated loss (310–410 °C) due to the degradation of the ammonium salt and the presence of agglomerated layers in the final morphology [23]. At temperatures above 500 °C, it can be observed only the inorganic fraction as residual mass. In Fig. 2, these systems showed a small change in the final inorganic residue (clay percentage in the real system), and have not provided changes in thermal stability of nanocomposites.

Figure 3 shows the XRD spectra of the pure MMT clay and nanocomposites of PP/MMT. The level of intercalation in clay powders and nanocomposites was determined by the measurement of the clay interlayer spacing (*d001*) from the 2θ position of the clay (*001*) diffraction peak using Bragg's law.

The MMT showed a characteristic peak at 2.6°, 2θ value corresponding to *d001* plane of clay. The PP/MMT samples showed this peak shifted to higher angles when compared to the neat MMT, suggesting that interlayer spacing tends to decrease into the PP matrix. Also, the peak at 6.9° suggests that a small percentage of the Na + MMT was not modified by the quaternary ammonium salt [24]. On the other hand, it is interesting to observe that PP containing 5 wt% MMT showed a sharp increase in peak intensity, and for those concentrations of 2 and 1 wt%, the clay peaks almost disappeared. This tendency suggests that the nanocomposites have not expanded or intercalated lattices. Low thermal stability of the clay intercalant

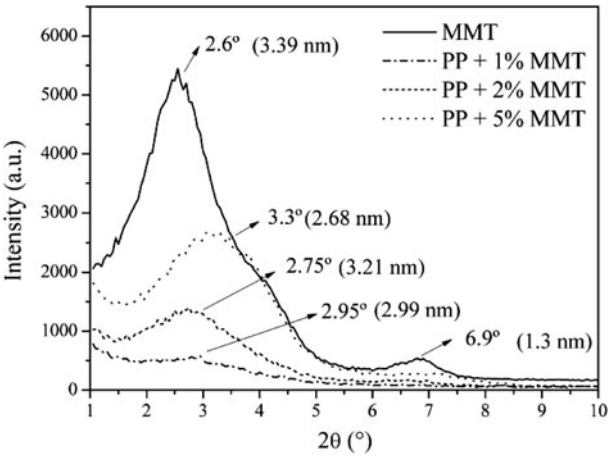

Fig. 3 XRD patterns of the MMT and PP/MMT nanocomposites

(organic ammonium salt) leading to clay collapse during compounding may be responsible for this interlayer spacing reduction [25].

Figure 4 shows the tensile properties for neat PP and PP/MMT nanocomposites.

There were no significant changes in Young's modulus values for neat PP and PP/MMT nanocomposites showing that MMT did not interfere in the PP stiffness as expected. Considering the neat PP, the nanocomposites showed only a fluctuation in the tensile strength. Besides, the deformation at break showed a slight increase, mainly to PP + 5 wt% MMT. This larger deformation suggests an improvement of toughness due to the dispersion of clay layers into the matrix. This behavior might be attributed to the tenacity of silicate layers which contributes to the modification

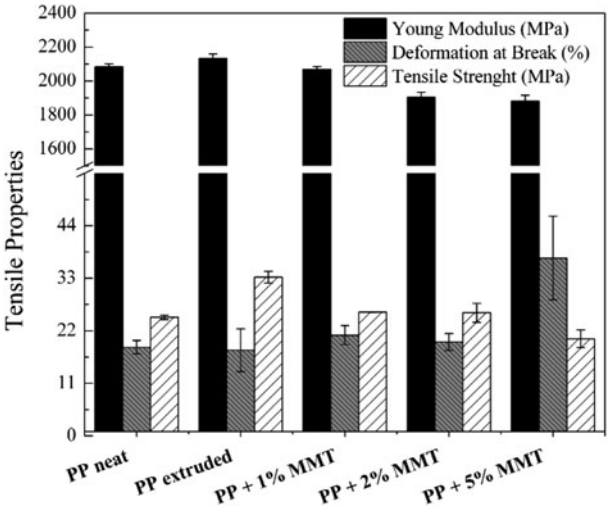

Fig. 4 Tensile properties of the neat PP and PP/MMT nanocomposites

Table 3 Impact properties of neat PP and PP/MMT nanocomposites

Samples	Impact strength (J m^{-1})	Impact energy (kJ m^{-2})
Neat PP	6.7 ± 0.4^{a}	2.1 ± 0.1^{a}
PP + 1% MMT	9.2 ± 1.4^{b}	2.9 ± 0.4^{b}
PP + 2% MMT	9.6 ± 1.3^{b}	3.0 ± 0.4^{b}
PP + 5% MMT	10.2 ± 0.5^{b}	3.2 ± 0.1^{c}

Means followed by the same letter within a column did not differ significantly ($P < 0.05$)

of PP phase structure or to the presence of partially immobilized polymer segments [7].

In this sense, a surprising increase in impact strength was observed (Table 3). The increase in impact strength was mainly related to the presence of clusters of clay in the PP matrix. These clusters may lead to the occurrence of additional mechanisms of energy absorption during fracture of the material, resulting in a higher impact resistance.

According to previous study of Castel et al. [22], the impact strength of polymers is mainly related to the dissipation mechanisms of energy flow by shear yielding and multiple crazing.

Figure 5 shows the micrographs of the PP/MMT nanocomposite with 2 and 5 wt% of MMT. These micrographs show some intercalated lamellae with particles distributed in the polymer matrix, with large and well-spaced clusters, demonstrating the process of exfoliation and the formation of nanocomposites. In addition, Fig. 5b shows morphology with a predominance of large MMT particles (pointed by the arrow) dispersed in the polymer matrix.

The concentration of MMT affected the ability of delamination and the filler was more evenly distributed into the PP matrix. Thus, the system containing 5 wt% MMT is more homogeneous than those lower contents; in relation to this, as for the greater the amount of nanoclay (higher volume of filler area), the better the distribution in the matrix. Figure 5c and d shows the formation of tactoids and some dispersed particles, pointed by arrows. According to some authors [26, 27], the tactoids consist of dark regions which represent stacked clay particles. The lighter regions represent the matrix of PP interspersed, or, the PP what lies between the lamellae of the clay (interlaced) during processing. According to the classification of Ray and Okamoto [9], this image can suggest that the nanocomposites presented a partially intercalated structure.

Corroborating to Benetti et al. [28], exfoliated clay layers are visible, along with tactoids. Inside the same tactoid, some layers are characterized by a stacking, very similar to that of pure MMT; some of them were more dispersed indicating that the intercalation of the polymer has occurred.

Analysis of permeability to oxygen and water vapor of nanocomposites PP/MMT as well for neat PP are presented in Table 4. The drop in oxygen permeability of these materials compared of the neat PP indicated that clay nanoparticles hinder the oxygen permeation through the PP matrix. According to Kester and Fennema [29], the process of permeation of vapors through the intermolecular spaces can be explained in three steps: (a) sorption and solubility of the permeant in the material

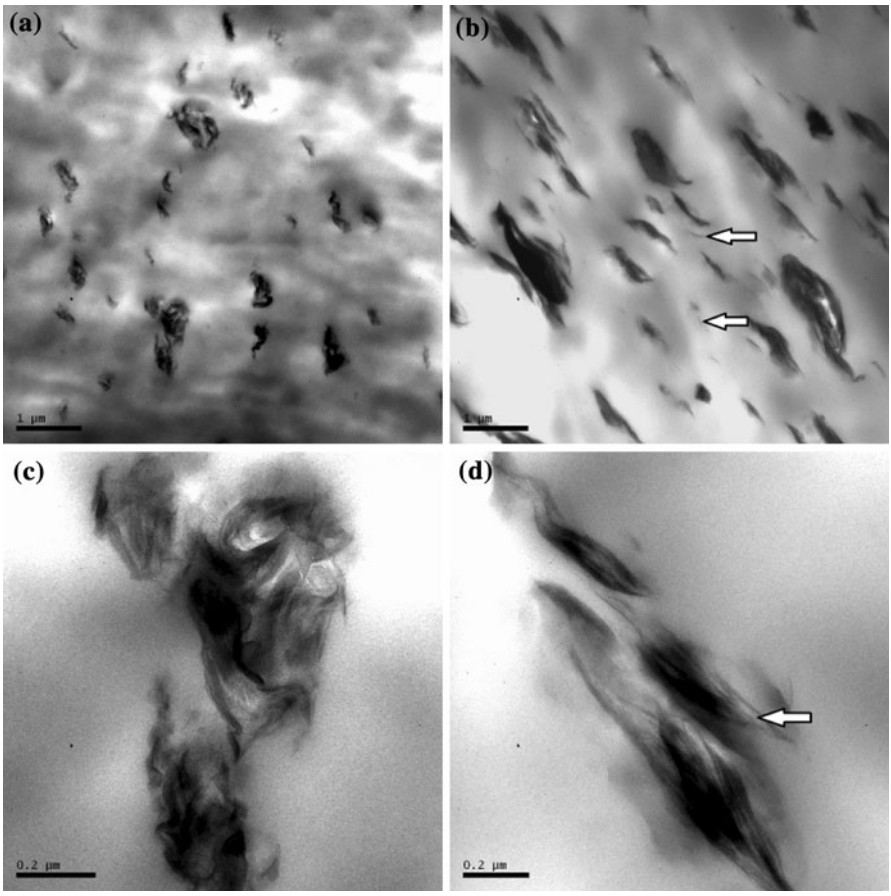

Fig. 5 TEM micrographs of PP/MMT nanocomposites: **a**, **c** 2 wt% and **b**, **d** 5 wt% of MMT

surface, (b) diffusion of permeating through the material by the action of gradient concentration, and (c) desorption and evaporation of the permeant on the other side of the material.

Other authors [30] suggest that the main mechanism for the flow of gases and vapor through the film, in the absence of cavities or cracks, is the molecular diffusion, which includes the open space between the segments of the polymer chains due to the oscillations of the segments, followed by displacement of the permeant into the empty space.

In food packaging, the packages must prevent or delay one or all stages involved to increase the shelf life of food and to increase the safety of the food to consumers. In this sense, nanofillers can act as a physical barrier that delays the passage of oxygen across the polymeric matrix. The resulting delay in the speed of diffusion allows the maintenance of food organoleptic properties thereby increasing its shelf life [2, 29, 31].

These results corroborates with the literature [2, 32–34] and shows that the decrease in oxygen permeability was caused by nanoparticles creating a physical

Table 4 Permeability of neat PP and PP/MMT nanocomposites

Samples	Permeability to O_2 (mm cm^3 m^{-2} dia^{-1})	Water vapor permeability (μm g m^{-2} dia^{-1})
Neat PP	89.9 ± 5.1^a	320 ± 28^a
PP + 1% MMT	88.2 ± 7.0^a	301 ± 20^a
PP + 2% MMT	85.3 ± 3.0^b	339 ± 8^a
PP + 5% MMT	81.8 ± 3.8^c	320 ± 14^a

Means followed by the same letter within a column did not differ significantly ($P < 0.05$)

obstacle that prevented oxygen absorption and slowing down its diffusion through the film, thereby increasing the distance that oxygen had to cover to cross through the film. In terms of water vapor permeability, the values remained nearly constant, probably due to its higher polarity.

SEM micrographs (Figs. 6, 7) show the film surface morphology, before and after contact with the orange juice. The squares represent the area of EDS analyses. SEM micrograph of a PP control film (without contact with orange juice) is shown in Fig. 6a. As expected, the surface of pure PP films is more homogeneous when compared with those of the PP/MMT nanocomposites (Fig. 6b, c), where a coarse appearance was observed in those films containing 1 and 5 wt% MMT.

Figure 7a shows the surface of the films of neat PP after contact with orange juice during 10 days. The surface of the PP films in contact with orange juice showed no changes compared with the original film (Fig. 7a). The SEM

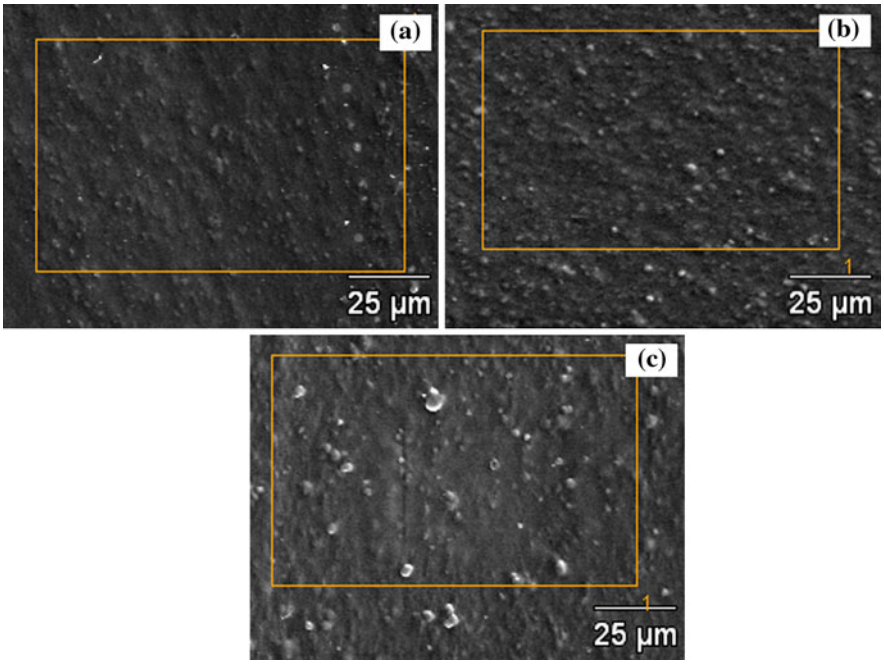

Fig. 6 SEM micrographs of the film packing samples: **a** neat PP, **b** PP 1 wt% MMT, and **c** PP 5 wt% MMT

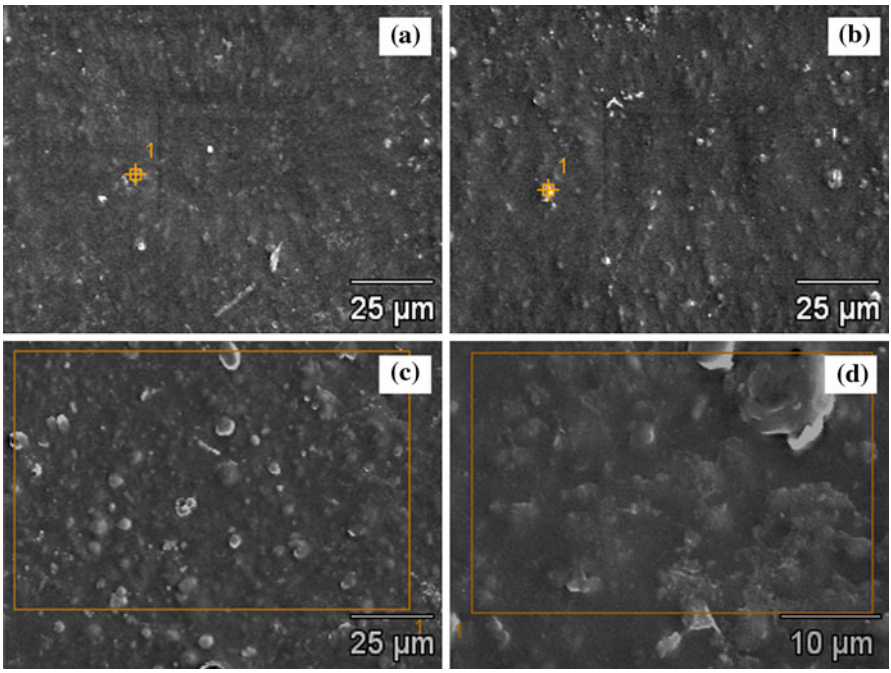

Fig. 7 SEM micrographs of the film packing samples after 10 days of contact with orange juice: **a** neat PP, **b** PP 1 wt% MMT, **c** and **d** PP 5 wt% MMT

Table 5 Relative elements concentration from EDS analyses of neat PP and PP/nanocomposites, before and after orange juice storage

Samples	Storage time (days)	Elements (atomic%)						
		C	Na	Al	Si	Mg	Fe	Au
Neat PP	0	13.17	ND	0.01	ND	ND	ND	86.82
Neat PP	10	16.39	ND	ND	ND	ND	ND	83.09
PP + 5% MMT	0	18.33	ND	0.19	0.62	ND	0.30	80.56
PP + 5% MMT	10	21.43	ND	0.16	0.76	ND	ND	77.65

micrographs of PP/MMT nanocomposites showed similar characteristics to that observed in films that had no contact with orange juice (Fig. 6b, c).

The PP with 5 wt% MMT (Fig. 7d) shows a micrograph with a larger magnification, in which a small amount of exfoliated lamellae can be seen.

With the addition of larger amounts of MMT it is possible to observe larger clusters of clay, which indicates a smaller interaction with PP. The X-ray spectrum emitted by a sample during SEM micrographs can be used to carry out a semi-quantitative chemical microanalysis. The X-ray spectra (not shown) of the PP control and PP nanocomposite, determined by the technique of EDS, resulted in the data of Table 5.

The addition of MMT in the PP matrix occasioned, as expected, the EDS signals related to the presence of silicon and aluminum, which are the main components of the MMT nanoparticles. The EDS analysis of PP shows only carbon and gold (from sputtering) instead.

After the storage period, the samples of PP and PP/MMT nanocomposites did not present changes in Al and Si contents, but only in Fe. This observation may suggest that most part of MMT nanoparticles were not eroded to the orange juice, but the iron counter-ions could have migrated instead.

Storage of orange juice quality in the nanocomposite packaging

The samples of orange juice showed an average density at 20 °C of 1.031 g mL^{-1}. There were no significant changes in the measured density values during 10 days. The value for soluble solids of the orange juice was 7.3 °Brix, and no significant variation as a function of storage time or type of packaging was observed. The established value for orange juice is 10.5 °Brix [35]. The °Brix value indicates the degree of fruit maturity at the instant of the juice preparation, in this way, the lowest value found may be associated to the use of not appropriated fruit during juice extraction [36]. The results of physical–chemical analyses in the freshly extracted orange juice, and those samples stored in packaging of neat PP and nanocomposite films for 1, 2, 3, 4, and 10 days are summarized in Table 6. In general, the titrable acidity and pH values were not changed regardless the type of package tested in the experiment. The pH decreased in the second day of storage when compared to fresh juice, before rising again in the final days of storage. Kaanane [37] found that titrable acidity does not change during storage of orange juice, because of a buffer system in the juice.

The total organic acids in the orange juice are formed by adding the citric and malic acids, found in a ratio of ~95:5. These two acids, mostly as salts, form a buffer with acid characteristics for the high amount of free acids that bind to the salts. This buffer system also explains the slightest variation in pH values [38]. These results can be related with those obtained by Kaanane [37], who also found no significant difference in pH of the juice during 14 weeks of storage. The authors attributed this slight variation in pH to the free acids present as a buffer.

The values for AA were found in accordance with the standards (minimum 25 mg 10^{-2} g^{-1}) [35], for all orange juice samples analyzed (Table 6). These values remained constant regardless the time of product storage or film package, suggesting that these films were appropriated. AA is usually degraded by the oxidative process, which is stimulated in the presence of light, oxygen, heat, peroxides, and enzymes [39]. In contrast to our findings, the overall AA reduction in juices has been associated to the non-barrier properties of packaging against oxygen [38] and the extent of storage time [40].

As can be visualized in Table 6, there was no significant difference in the levels of reducing, non-reducing, and total sugars in the samples at different days of storage. The average values of reducing sugars ranged from 2.50 to 2.77 in the samples of PP/MMT. Some of the observed levels of reducing sugars are higher than non-reducing sugars; this fact is explained because fructose (reducing sugar) is

Table 6 Physical and chemical characteristics of orange juice stored for 10 days in packs of PP and nanocomposites

Samples	Storage time (days)	ATT (% citric acid)	pH	AA (mg/%)	Reducing sugars (g glucose/100 g)	Total sugars (%)	Non-reducing sugars (g saccharose/100 g)
Fresh juice	0	0.82 ± 0.06^{a}	3.79 ± 0.01^{a}	53.31 ± 0.36^{a}	2.62 ± 0.02^{a}	5.09 ± 0.06^{a}	2.34 ± 0.04^{a}
Neat PP		0.81 ± 0.06^{a}	3.65 ± 0.01^{b}	57.60 ± 2.50^{b}	2.76 ± 0.00^{b}	5.27 ± 0.07^{b}	2.39 ± 0.06^{a}
PP + 1% MMT	1	0.79 ± 0.00^{a}	3.56 ± 0.16^{b}	52.01 ± 0.77^{c}	2.77 ± 0.02^{b}	5.42 ± 0.00^{c}	2.51 ± 0.02^{b}
PP + 2% MMT		0.78 ± 0.00^{a}	3.61 ± 0.00^{b}	52.09 ± 0.18^{c}	2.76 ± 0.00^{b}	5.32 ± 0.14^{b}	$2.43 \pm 0.13^{a,b}$
PP + 5% MMT		0.74 ± 0.00^{b}	3.62 ± 0.11^{b}	51.29 ± 0.24^{c}	2.73 ± 0.00^{c}	5.27 ± 0.07^{b}	$2.41 \pm 0.06^{a,b}$
Neat PP		0.91 ± 0.00^{c}	3.46 ± 0.01^{c}	57.30 ± 1.25^{b}	2.66 ± 0.00^{a}	4.78 ± 0.06^{d}	2.02 ± 0.06^{c}
PP + 1% MMT	2	0.91 ± 0.00^{c}	3.36 ± 0.04^{d}	51.92 ± 0.65^{c}	2.64 ± 0.00^{a}	4.96 ± 0.06^{a}	2.20 ± 0.06^{d}
PP + 2% MMT		0.85 ± 0.00^{a}	3.21 ± 0.01^{d}	53.90 ± 0.00^{a}	2.59 ± 0.06^{a}	5.00 ± 0.00^{a}	$2.29 \pm 0.06^{a,d}$
PP + 5% MMT		0.84 ± 0.00^{a}	3.16 ± 0.03^{e}	56.21 ± 1.01^{b}	2.39 ± 0.03^{d}	4.96 ± 0.06^{a}	$2.44 \pm 0.09^{a,b}$
Neat PP		0.84 ± 0.00^{a}	3.63 ± 0.00^{b}	52.64 ± 2.61^{c}	2.49 ± 0.02^{e}	5.14 ± 0.07^{a}	2.52 ± 0.08^{b}
PP + 1% MMT	3	0.89 ± 0.00^{c}	3.63 ± 0.01^{b}	59.28 ± 0.36^{d}	2.51 ± 0.02^{e}	$5.19 \pm 0.14^{a,b}$	2.55 ± 0.12^{b}
PP + 2% MMT		0.84 ± 0.00^{a}	3.62 ± 0.01^{b}	54.03 ± 1.13^{a}	2.50 ± 0.00^{e}	$5.19 \pm 0.00^{a,b}$	2.55 ± 0.00^{b}
PP + 5% MMT		0.87 ± 0.00^{a}	3.63 ± 0.00^{b}	60.50 ± 7.43^{d}	2.51 ± 0.02^{e}	5.09 ± 0.00^{a}	$2.45 \pm 0.02^{a,b}$
Neat PP		0.87 ± 0.00^{a}	3.69 ± 0.02^{f}	56.88 ± 9.33^{b}	2.71 ± 0.02^{c}	5.14 ± 0.07^{a}	2.31 ± 0.05^{a}
PP + 1% MMT	4	0.89 ± 0.00^{c}	3.69 ± 0.01^{f}	56.76 ± 8.79^{b}	2.61 ± 0.02^{a}	5.29 ± 0.14^{b}	2.55 ± 0.12^{b}
PP + 2% MMT		0.89 ± 0.00^{c}	3.72 ± 0.03^{f}	57.43 ± 10.22^{b}	2.55 ± 0.00^{a}	5.00 ± 0.13^{a}	$2.33 \pm 0.12^{a,d}$
PP + 5% MMT		0.88 ± 0.00^{a}	3.72 ± 0.01^{f}	60.75 ± 10.04^{d}	2.59 ± 0.00^{a}	5.61 ± 0.00^{e}	2.87 ± 0.00^{e}
Neat PP		0.89 ± 0.01^{c}	3.72 ± 0.01^{f}	54.57 ± 4.99^{a}	2.58 ± 0.02^{a}	5.09 ± 0.00^{a}	2.38 ± 0.02^{a}
PP + 1% MMT	10	0.91 ± 0.01^{c}	3.72 ± 0.00^{f}	57.51 ± 3.33^{b}	2.59 ± 0.03^{a}	5.50 ± 0.16^{c}	2.76 ± 0.18^{e}
PP + 2% MMT		0.92 ± 0.02^{c}	3.73 ± 0.01^{f}	57.85 ± 2.14^{b}	2.58 ± 0.02^{a}	5.50 ± 0.16^{c}	2.77 ± 0.16^{e}
PP + 5% MMT		0.91 ± 0.00^{c}	3.73 ± 0.00^{f}	57.55 ± 4.46^{b}	2.56 ± 0.02^{a}	5.45 ± 0.08^{c}	2.74 ± 0.06^{e}

Means followed by the same letter within a column did not differ significantly ($P < 0.05$)

the predominant sugar in the orange, while sucrose is present in small quantities [41]. The maximum value for total sugars of natural orange established by the regulation is 13.0 g 10^{-2} g^{-1} [35].

According to the results in Table 6, none of the samples analyzed showed a total sugar content above the stipulated amount. It can be also noted that no significant changes were observed among the samples packed in different materials. The mean levels of total sugars varied from 4.78 to 5.61.

The results of microbiological analysis indicated the absence of total and fecal coliforms for all analyzed samples. These results are according to Brazilian law, which establishes a maximum of 10 MPN mL^{-1} to fecal coliforms in 25 mL sample of fruit juice [42]. The absence of coliforms may be associated with the fact that juice production and storage was developed under good manufacture practices.

Figure 8a shows the results of the microbial counts of orange juice stored during 10 days under refrigeration (4 °C). For two types of packaging (2 and 5 wt% MMT), there was a reduction in the total counts of bacteria during the first 24 h of storage.

From this point on, the microbial counts had been stabilized and increased for some samples. The results of this analysis are consistent with those reported by some authors [43, 44], which agrees that microbial counts may decrease during the first hours of refrigeration storage. Furthermore orange juice stored at 4 °C in nanocomposite LDPE films containing Ag and ZnO nanoparticles showed microbial stability up to 28 days, but yeast, molds, and bacteria exhibit different levels of susceptibility antimicrobial to nanoparticles [44]. Moreover, the microbial population has increased as the time storage increased to 56 days in different test packages, indicating the limited effect of long storage time on natural orange juice preservation. Figure 8b indicates the small variation in counts of yeasts and molds regardless of type of packaging. The values were between 3.0 and 3.7 log UFC mL^{-1} for up to 10 days, indicating that nanocomposite films could be useful materials for juice packaging. The greater agglomeration of nanoparticles observed in the films with increased MMT concentration (Fig. 5a, b) did not influence the microbiological quality of the orange juice. Yeast and molds are better adapted to

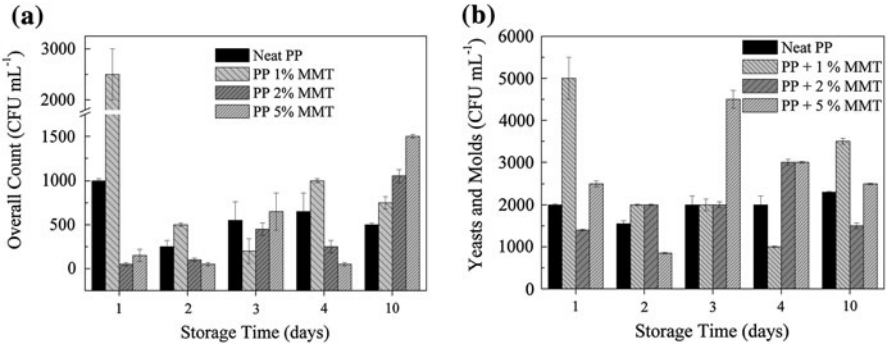

Fig. 8 **a** Overall and **b** yeasts and molds counts for orange juice stored in PP packaging films with different concentrations of MMT. Initial counts of fresh juice were 10^3 CFU mL^{-1} and 7.2×10^3 CFU mL^{-1} for overall and yeast/mold counts, respectively. All samples were stored for 10 days at 4 °C

orange juice under refrigeration than bacteria, which is in agreement with the literature [43, 45]. Moreover, yeasts are recognized as the most significant group of microorganisms associated with spoilage of fruit juices [46].

The rough surface observed in PP/MMT nanocomposite films (Fig. 7a–c), could support the adhesion of microbial cells, since the presence of irregularities of polymeric surfaces promotes bacterial adhesion and biofilm deposition whereas the ultra-smooth surface does not favor adhesion [47]. However, no adhered microorganisms were observed by SEM analysis of the films after 10-day storage. In accordance, the greater agglomeration of nanoparticles observed in the films with increased MMT concentration did not influence the microbiological quality of the orange juice.

Conclusions

PP/MMT nanocomposites were prepared by melt processing in a twin-screw extruder up to 5 wt%, to develop food package films with enhanced barrier and mechanical properties. Despite the fact that no significant changes in nanocomposites tensile properties with the MMT addition were observed, the impact strength presented a substantial enhancement and the rigidity as well. SEM and TEM micrographs revealed certain homogeneity in the MMT dispersion, showing some exfoliated lamellae in the PP matrix. Regarding the package efficacy, the orange juice quality was maintained after 10 days of storage, as evaluated by selected parameters. The presence of coliforms was not detected; the mold count decreased after 24 h of storage. Besides, MMT has shown some capacity to improve oxygen barrier properties. Concluding, this study seems to clarify a little more the claimed efficiency of nanocomposites as food packing materials.

Acknowledgments The authors are grateful to Dr. Mauro Oviedo from Braskem S/A for the permeability analyses. The authors also wish to thank CAPES, CNPq, PRONEX/FAPERGS for financial support.

References

1. Silvestre C, Duraccio D, Cimmino S (2011) Food packaging based on polymer nanomaterials. Prog Polym Sci 36:1766–1782. doi:10.1016/j.progpolymsci.2011.02.003
2. Pereira D, Losada PP, Angulu I, Greaves W, Cruz JM (2009) Development of a polyamide nanocomposite for food industry: morphological structure, processing, and properties. Polym Comp 30:436–444. doi:10.1002/pc.20574
3. Brody AL, Bugusu B, Han JH, Sand CK, McHugh TH (2008) Innovative food packaging solutions. J Food Sci 73:107–116. doi:10.1111/j.1750-3841.2008.00933.x
4. Fu X, Qutubuddin S (2001) Polymer–clay nanocomposites: exfoliation of organophilic montmorillonite nanolayers in polystyrene. Polymer 42:807–813. doi:10.1016/s0032-3861(00)00385-2
5. Lan T, Kaviratna PD, Pinnavaia TJ (1994) Clay-reinforced epoxy nanocomposites. Chem Mater 6:2216–2219. doi:10.1021/cm00048a006
6. Kelly P, Akelah A, Qutubuddin S, Moet A (1994) Reduction of residual stress in montmorillonite/epoxy compounds. J Mater Sci 29:2274–2280. doi:10.1007/bf00363414
7. Santos KS, Liberman SA, Oviedo MAS, Mauler RS (2009) Optimization of the mechanical properties of polypropylene-based nanocomposite via the addition of a combination of organoclays. Composites Part A 40:1199–1209. doi:10.1016/j.compositesa.2009.05.009

8. Hussain F, Hojjati M, Okamoto M, Gorga RE (2006) Review article: polymer-matrix nanocomposites, processing, manufacturing, and application: an overview. J Compos Mater 40:1511–1575. doi:10.1177/0021998306067321
9. Sinha Ray S, Okamoto M (2003) Polymer/layered silicate nanocomposites: a review from preparation to processing. Prog Polym Sci 28:1539–1641. doi:10.1016/j.progpolymsci.2003.08.002
10. Calcagno CIW, Mariani CM, Teixeira SR, Mauler RS (2007) The effect of organic modifier of the clay on morphology and crystallization properties of PET nanocomposites. Polymer 48:966–974. doi:10.1016/j.polymer.2006.12.044
11. Paul DR, Robeson LM (2008) Polymer nanotechnology: nanocomposites. Polymer 49:3187–3204. doi:10.1016/j.polymer.2008.04.017
12. Esteves ACC, Barros-Timmons A, Trindade T (2004) Nanocompósitos de matriz polimérica: estratégias de síntese de materiais híbridos. Quim Nova 27:798–806
13. García-Lopez D, Picazo O, Merino JC, Pastor JM (2003) Polypropylene–clay nanocomposites: effect of compatibilizing agents on clay dispersion. J Eur Polym 39:945–950. doi:10.1016/s0014-3057(02)00333-6
14. Zhu L, Xanthos MJ (2004) Effects of process conditions and mixing protocols on structure of extruded polypropylene nanocomposites. J Appl Polym Sci 93:1891–1899. doi:10.1002/app.20658
15. Sheng N, Boyce MC, Parks DM, Rutledge GC, Abes JI, Cohen RE (2004) Multiscale micromechanical modeling of polymer/clay nanocomposites and the effective clay particle. Polymer 45:487–506. doi:10.1016/j.polymer.2003.10.100
16. Lertwimolnun W, Vergnes B (2005) Influence of compatibilizer and processing conditions on the dispersion of nanoclay in a polypropylene matrix. Polymer 46:3462–3471. doi:10.1016/j.polymer.2005.02.018
17. Picard E, Gérard JF, Espuche E (2008) Water transport properties of polyamide 6 based nanocomposites prepared by melt blending: on the importance of the clay dispersion state on the water transport properties at high water activity. J Membr Sci 313:284–295. doi:10.1016/j.memsci.2008.01.011
18. Tidjani A, Wald O, Pohl M-M, Hentschel MP, Schartel B (2003) Polypropylene–graft–maleic anhydride-nanocomposites: I—Characterization and thermal stability of nanocomposites produced under nitrogen and in air. Polym Degrad Stab 82:133–140. doi:10.1016/s0141-3910(03)00174-5
19. Association of Official Analytical Chemists—AOAC (1995) Official methods of analysis
20. American Public Health Association—APHA (1992) Compendium of methods for the microbiological examination of foods 3: 1219
21. Lim JW, Hassan A, Rahmat AR, Wahit MU (2006) Morphology, thermal and mechanical behavior of polypropylene nanocomposites toughened with poly(ethylene-co-octene). Polym Int 55:204–215. doi:10.1002/pi.1942
22. Castel CD, Ovideo MAS, Liberman SA, Oliveira RVB, Mauler RS (2011) Solvent-assisted extrusion of polypropylene/clay nanocomposites. J Appl Polym Sci 121:389–394. doi:10.1002/app.33605
23. Lewin M, Pearce EM, Levon K, Mey-Marom A, Zammarano M, Wilkie CA, Jang BN (2006) Nanocomposites at elevated temperatures: migration and structural changes. Polym Adv Technol 17:226–234. doi:10.1002/pat.684
24. Kim NH, Malhotra SV, Xanthos M (2006) Modification of cationic nanoclays with ionic liquids. Microporous Mesoporous Mater 96:29–35. doi:10.1016/j.micromeso.2006.06.017
25. Perrin-Sarazin F, Ton-That MT, Bureau MN, Denault J (2005) Micro- and nano-structure in polypropylene/clay nanocomposites. Polymer 46:11624–11634. doi:10.1016/j.polymer.2005.09.076
26. Rodrigues AW, Brasileiro MI, Araújo WD, Araújo EM, Neves GA, Melo TJA (2007) Desenvolvimento de nanocompósitos polipropileno/argila bentonita brasileira: I tratamento da argila e influência de compatibilizantes polares nas propriedades mecânicas. Polim Ciên Tecnol 17:219–227
27. Dong Y, Bhattacharyya D (2008) Effects of clay type, clay/compatibiliser content and matrix viscosity on the mechanical properties of polypropylene/organoclay nanocomposites. Composites Part A 39:1177–1191. doi:10.1016/j.compositesa.2008.03.006
28. Benetti EM, Causin V, Marega C, Marigo A, Ferrara G, Ferraro A, Consalvi M, Fantinel F (2005) Morphological and structural characterization of polypropylene based nanocomposites. Polymer 46:8275–8285. doi:10.1016/j.polymer.2005.06.056
29. Kester JJ, Fennema O (1986) Edible films and coatings: a review. Food Technol 40:47–59
30. Mali S, Grossmann MVE, Yamashita F (2010) Starch films: production, properties and potential of utilization. Semina: Ciências Agrárias 31:137–156

31. Duncan TV (2011) Applications of nanotechnology in food packaging and food safety: barrier materials, antimicrobials and sensors. J Colloid Interface Sci 363:1–24. doi:10.1016/j.jcis.2011.07.017
32. Mittal V (2008) Mechanical and gas permeation properties of compatibilized polypropylene-layered silicate nanocomposites. J Appl Polym Sci 107:1350–1361. doi:10.1002/app.26952
33. Osman MA, Mittal V, Suter UW (2007) Poly(propylene)-layered silicate nanocomposites: gas permeation properties and clay exfoliation. Macromol Chem Phys 208:68–75. doi:10.1002/macp.200600444
34. Ali Dadfar SM, Alemzadeh I, Reza Dadfar SM, Vosoughi M (2011) Studies on the oxygen barrier and mechanical properties of low density polyethylene/organoclay nanocomposite films in the presence of ethylene vinyl acetate copolymer as a new type of compatibilizer. Mater Des 32:1806–1813. doi:10.1016/j.matdes.2010.12.028
35. Brasil (1987) Ministério da Agricultura e do Abastecimento. Portaria DINAL número 01 de 28 de janeiro de 1987. Available at: www.anvisa.gov.br. Accessed Jan 2010
36. Ruschel CK, Carvalho HH, Souza RB, Tondo EC (2001) Qualidade microbiológica e físico-química de sucos de laranja comercializados nas vias públicas de Porto Alegre/RS. Ciên Tecnol Aliment 21:94–97
37. Kaanane A, Kane D, Labuza TP (1988) Time and temperature effect on stability of moroccan processed orange juice during storage. J Food Sci 53:1470–1473. doi:10.1111/j.1365-2621.1988.tb09301.x
38. Kimball DA (1999) Citrus processing: a complete guide. Aspen Publishers, New York
39. Plaza L, Sánchez-Moreno C, Elez-Martinez P, Ancos B, Matín-Belloso O, Cano MP (2006) Effect of refrigerated storage on vitamin C and antioxidant activity of orange juice processed by high-pressure or pulsed electric fields with regard to low pasteurization. Eur Food Res Technol 233:487–493. doi:10.1007/s00217-005-0228-2
40. Martín-Diana AB, Rico D, Barat JM, Barry-Ryan C (2009) Orange juices enriched with chitosan: optimisation for extending the shelf-life. Innov Food Sci Emerg Technol 10:590–600. doi:10.1016/j.ifset.2009.05.003
41. Branco IG, Gasparetto CA (2003) Aplicação da metodologia de superfície de resposta para o estudo do efeito da temperatura sobre o comportamento reológico de misturas ternárias de polpa de manga e sucos de laranja e cenoura. Ciên Tecnol Aliment 23:166–171
42. Ministry of Health, Brazil (2001) RDC n° 12, de 02/01/2001. Available: http://www.anvisa.org.br. Accessed 20 Aug 2011
43. Sadler GD, Parish ME, Wicker L (1992) Microbial, enzymatic, and chemical changes during storage of fresh and processed orange juice. J Food Sci 57:1187–1197. doi:10.1111/j.1365-2621.1992.tb11295.x
44. Emamifar A, Kadivar M, Shahedi M, Soleimanian-Zad S (2010) Evaluation of nanocomposite packaging containing Ag and ZnO on shelf life of fresh orange juice. Innov Food Sci Emerg Technol 11:742–748. doi:10.1016/j.ifset.2010.06.003
45. Tournas VH, Heeres J, Burgess L (2006) Moulds and yeasts in fruit salads and fruit juices. Food Microbiol 23:684–688. doi:10.1016/j.fm.2006.01.003
46. Wareing P, Davemport RR (2005) Chemistry and technology of soft drinks and fruit juices. Blackwell, Oxford, pp 279–297
47. Katsikogianni M, Missirlis YF (2004) Concise review of mechanisms of bacterial adhesion to biomaterials and of techniques used in estimating bacteria–material interactions. Eur Cells Mater 8:37–57